An Improved Active Zero Voltage Switching Assisting Circuit with Lower dv/dt for DC-DC Series Resonant Converter with Constant Input Current

Tarak Saha, Hongjie Wang, Baljit Riar and Regan Zane
ECE Department
Utah State University
Logan, UT – USA 84341
e-mail: tarak.saha@aggiemail.usu.edu

***Abstract*— With a constant current dc power distribution system, the input voltage of each series connected power converter module varies with the load. Achieving zero voltage switching (ZVS) for the converter using passive techniques becomes a challenging and difficult task with the wide variation in the load that also changes the input voltage. Therefore, an active assisting method that adapts to the varying input voltage is needed for achieving ZVS with good efficiency over the load range. Traditional active ZVS assistance techniques either operates with higher rms currents in the main switches and the ZVS assisting branch, which further result in higher conduction losses, or result in hard switching of assisting switches, which result in high EMI due to high *dv/dt*, at full DC bus voltage. In this paper, an active ZVS assisting circuit is proposed which operates with low rms currents in the assisting branch with lower EMIs due to *dv/dt* in the assisting branch. The proposed technique is experimentally verified through testing of a series resonant converter whose input is connected to a 1 A current source and output current is regulated at 0.33 A for a full load of 250 W, operating at a switching frequency of 250 kHz.**

Keywords—zero voltage switching, resonant converter, dc distribution, constant current distribution, active ZVS

I. INTRODUCTION

Resonant converters have gained wide popularity due to their advantages of high power density, soft switching ability, low EMI, high reliability. Therefore these converters are widely used in dc distribution systems [1-2], wireless power transfer systems [3], and battery management systems [4-5]. With the advent of modern high speed wide band gap devices, operating frequency of power converters is increasing and thus soft-switching of the devices has become important for reliable and efficient power conversion [6, 14]. With the fixed switching frequency, series resonant converters (SRCs), which is one of the popular converters due to its low component count, cannot operate with zero voltage switching (ZVS) for the entire range of load and input voltage and, as a result, ZVS assisting circuit are needed to accomplish soft switching [14-16] in order to have efficient power conversion.

For SRCs with constant input DC voltage, various passive [7-9] and active ZVS assisting techniques [10-14] are proposed in literature. Passive ZVS assisting methods have advantages, such as simple to implement and small volume that is occupied by the components. However, achieving ZVS of switches using passive techniques fail to maintain high efficiency for a wide operating range of loads. Active ZVS assisting techniques can easily overcome this limitation by controlling the assisting current. Active assisting techniques used in [13-14] achieve ZVS for both the main switches and the assisting/auxiliary switches. However, it should be noted that depending on operating point, the rms current in the assisting branch as well as the main switches can be high, which can reduce the converter efficiency. In [10-12], authors presented several techniques to reduce the conduction losses in the assisting circuit, but these techniques do not have ZVS for the auxiliary switches. These techniques result in additional losses due to the energy that is stored in devices' output capacitance and also result in high *dv/dt* at the turn on of the auxiliary switches, especially at higher input voltages.

In this paper, an active ZVS assisting circuit is proposed that achieves ZVS of the main leg switches with low rms current in both the main switching leg as well as the assisting branch with low *dv/dt* of the assisting switches. The topology and analysis presented in this digest is for a DC-DC SRC with constant current input where the input voltage varies with the load. This topology is suitable for undersea applications as presented in [2], and its ZVS requirements vary over wide range, based on the load. Section II covers the basic steady state operation of the converter which is needed to analyze the ZVS assistance requirement. In section III, the proposed ZVS assisting circuit and its variants are presented. Operation of the proposed circuit is explained with its equivalent circuit, along with desired ratings of the circuit components. Hardware results are presented in section IV for an SRC operating at 250 kHz from a constant input source of 1 A with its output regulated at 0.33 A for a load up to 250 W.

The work presented in this paper was sponsored by the Raytheon Company through the Utah State University Power Electronics Lab (UPEL).

II. Steady State Analysis of SRC with Constant Current Input

The SRC circuit topology operating from constant current input is shown in Fig. 1. On the primary side of the converter, MOSFETs Q_1 – Q_4 forms the DC-AC inverting stage, that applies an output voltage (v_{AB}) across a resonant tank constituted by an inductor L_r and a capacitor C_r. The output side of the converter is a diode half bridge voltage doubler with a capacitive filter, which rectifies and filters the AC output of the 1:n isolation transformer. The power delivered to a load (R_{load}) is obtained from a DC constant input current source (I_g). The converter design and its steady state analysis are presented in [1-2]. As presented in [2], the SRC is operated at a switching frequency (f_s) that is equal to the resonant frequency (f_o) of the tank, resulting in a constant current behavior at the output irrespective of the load resistance R_{load}. This current source nature of the converter reduces an effort required from the controller to regulate the load current. From [2], the steady state DC input voltage (V_{in}), DC output voltage (V_{out}) and DC output current (I_{out}) of the converter can be given as

$$V_{in} = \frac{I_g R_{load}}{4n^2 \sin^2(\frac{\alpha}{2})}, \quad (1)$$

$$V_{out} = \frac{I_g R_{load}}{2n \sin(\frac{\alpha}{2})}, \quad (2)$$

$$I_{out} = \frac{I_g}{2n \sin(\frac{\alpha}{2})}, \quad (3)$$

where, α is the phase shift angle between leg A and leg B of the converter, with leg A voltage leading that of leg B. Symmetric phase shift modulation technique with constant switching frequency is employed for the primary side inverter. These steady state quantities are needed to evaluate ZVS assistance requirement for each of the switching legs. From (3) it can be seen that the output behaves as constant current, independent of load resistance (R_{load}), for a given input current (I_g), transformer turns ratio (n) and phase shift angle (α). So, for a regulated output current scenario, phase shift angle (α) is constant, under ideal circumstances. With constant α, I_g and n, input voltage (V_{in}) varies linearly with R_{load}. This brings in wide variation in DC bus voltage of the primary side inverter and hence passive ZVS assisting techniques cannot achieve ZVS of all switches for the entire load range without compromising heavy load efficiency.

In addition to the main power processing circuit in Fig. 1, a ZVS assisting circuit is connected between switch node A and DC bus negative terminal. Based on the analysis presented in [9, 14], only the leading leg (leg A) needs ZVS assistance whereas the lagging leg achieves natural ZVS by the tank current. Hence, in the remaining part of this paper, only leg A of the converter and its assisting circuit is shown.

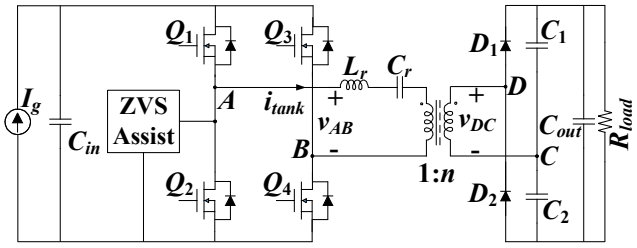

Fig. 1. SRC circuit topology with ZVS assisting circuit, operating from constant current input.

III. ZVS Assisting Circuit

The proposed basic ZVS assisting circuit which is similar in operation with the assisting circuit mentioned in [10] is shown in Fig. 2(a). Capacitance C_{D1} and C_{D2} represent the output capacitor of MOSFETs Q_1 and Q_2, respectively. Inductor L_{ZVS} provides the reactive current needed for ZVS and capacitor C_{ZVS} blocks the DC voltage at switch node A. Active switches S_1 and S_2 are turned on such that they create a short duration triangular pulse around the switching instant of main MOSFETs. Prior to the gate turn on of the main

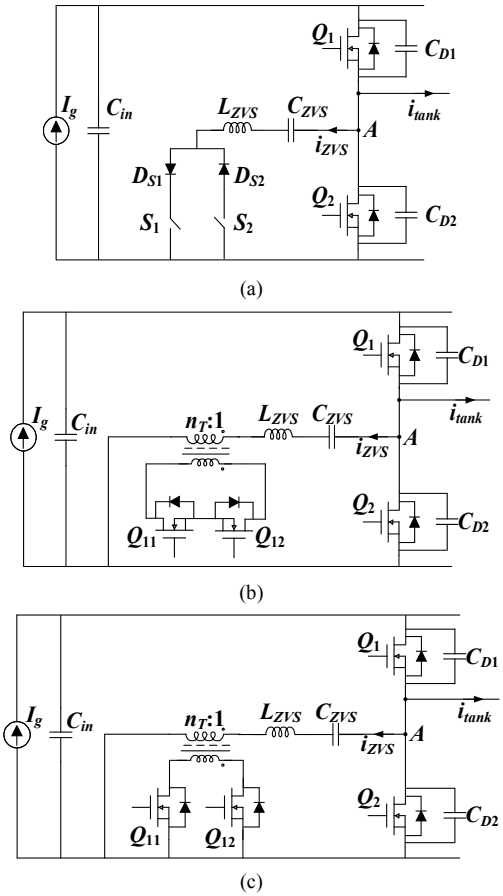

Fig. 2. Proposed basic ZVS assisting circuit diagram (a). Modified configurations of the proposed ZVS assisting circuit: (b) with floating gate driver for the auxiliary MOSFETs (c).with ground referenced gate driver for the auxiliary MOSFETs.

MOSFETs, these pulses create a net current at switch node A in an appropriate direction to charge/discharge the effective capacitance at the node. Diodes D_{S1} and D_{S2} ensure zero current turn on and off of auxiliary switches S_1 and S_2. It should be noted that even though the auxiliary switches change state with zero current, energy stored in the output capacitance (C_{oss}) of the devices is discharged in the device while turning on. This energy lost increases exponentially as the operating DC bus voltage increases and also creates large dv/dt related EMI, at device turn on. Therefore, this circuit is not favorable for the SRC with the constant input current, because its DC bus voltage increases with the load where ZVS is mostly needed.

In order to overcome these limitations, a modified ZVS assisting circuit is proposed in Fig. 2(b) where the auxiliary switches are transferred to the low voltage side of an auxiliary transformer and, thus, reduces the turn on voltage magnitude across the auxiliary switches. Leakage inductance of the transformer is utilized as ZVS assisting inductance, L_{ZVS}. Since the voltage stress across the auxiliary switches are lower, a low cost silicon based MOSFET can be used to realize these switches. Capacitor C_{ZVS} works as a DC blocking capacitor in the circuit whose operating voltage is $0.5V_{in}$. The ZVS assisting circuit of Fig. 2(b) can alternately be realized by circuit shown in Fig. 2(c) where the auxiliary MOSFETs gate driver is referenced to ground. However, one major drawback of these circuit realizations is reverse recovery effect of the body diodes of auxiliary MOSFETs which can introduce high frequency oscillations near the zero crossing of ZVS assisting current and thus produce more EMI. A schottky diode with lower on state voltage drop, compared to the body diode of auxiliary MOSFETs, can help reducing these oscillations.

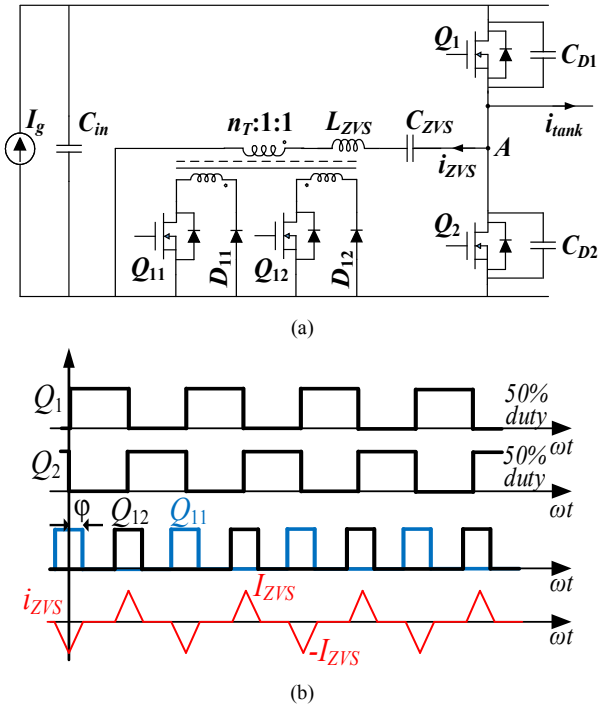

Fig. 3. Proposed ZVS assisting circuit with 3 winding auxiliary transformer (a). Ideal PWM drive and operating waveform of the active ZVS assisting circuit (b).

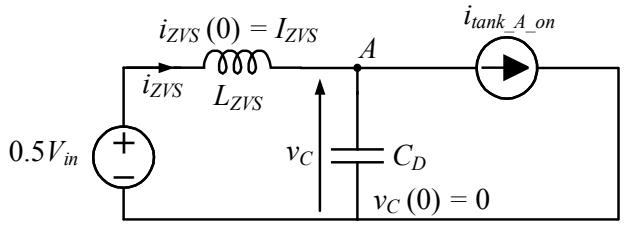

Fig. 4. Equivalent circuit during resonant transition.

Because of these disadvantages, the circuit configuration presented in Fig. 3(a) is used as the ZVS assisting circuit for the SRC and the analysis presented here on is for the circuit proposed in Fig. 3(a)

A three winding transformer is used in the circuit shown in Fig. 3(a) so that both the gates of auxiliary switches, which have a common ground, can be driven without isolation. And the diodes D_{11} and D_{12} are selected to be schottky diodes so that there is no reverse recovery effect.

The drive signals for the auxiliary switches are shown in Fig. 3(b) along with the ideal waveform of i_{ZVS}. Angle φ controls the amplitude of i_{ZVS} (I_{ZVS}) which is dependent on V_{in}, L_{ZVS} and operating angular switching frequency ω_s, related by

$$\varphi = \frac{2\omega_s L_{ZVS} I_{ZVS}}{V_{in}}. \tag{4}$$

The actual peak value of i_{ZVS} will be higher than I_{ZVS} and is determined by the resonating circuit formed by L_{ZVS} and the capacitor (C_D) at switch node A [17], as shown in Fig. 4.

The equivalent circuit during the dead time (t_{db}) between Q_1 and Q_2 is shown in Fig. 4. From the equivalent circuit shown in Fig. 4, the inductor current and capacitor voltage dynamics, during the resonant transition, are be given by

$$L_{ZVS}\frac{di_{ZVS}}{dt} = 0.5V_{in} - v_C, \tag{5}$$

$$C_D\frac{dv_C}{dt} = i_{ZVS} - i_{tank\_A\_on}, \tag{6}$$

where, C_D is the total capacitance at switch node A, due to the output capacitance of MOSFETs Q_1 and Q_2, including any board parasitic capacitance present across these devices [14, 17]. In (6), $i_{tank\_A\_on}$ is the current out of the half bridge switching node A, at the turn off instant of Q_2 and is assumed to have negligible variation during the resonant transition at the switch node. The value of $i_{tank\_A\_on}$ can be found through the time domain analysis of tank current, as presented in [8]. Since the input DC voltage varies with the load, the analysis from [8] has to be performed for the range of load. A circuit simulation can also be performed to know the value of $i_{tank\_A\_on}$ at different load. The above equations are also valid for the transition from turning off Q_1 to turning on Q_2 transition as well, due to half wave symmetry in the circuit. The solutions to (5) and (6) can be given by

$$i_{ZVS}(t)=\frac{V_{in}}{2Z_{oa}}\sin(\omega_{oa}t) + (I_{ZVS}-i_{tank\_A\_on})\cos(\omega_{oa}t)+i_{tank\_A\_on}, \quad (7)$$

$$v_C(t)=0.5V_{in}(1-\cos(\omega_{oa}t)) + Z_{oa}(I_{ZVS}-i_{tank\_A\_on})\sin(\omega_{oa}t), \quad (8)$$

where, Z_{oa} and ω_{oa} are defined as

$$Z_{oa}=\sqrt{\frac{L_{ZVS}}{C_D}}, \qquad \omega_{oa}=\frac{1}{\sqrt{L_{ZVS}C_D}}. \quad (9)$$

From (7) and (8), we can find out whether, with a starting current of I_{ZVS} in L_{ZVS} i.e. $i_{ZVS}(0) = I_{ZVS}$, the voltage across C_D can make a transition from initial voltage of 0 V to a final voltage greater than or equal to V_{in} within dead time t_{db}, to ensure that the body diode of Q_1 turns on before its gate pulses are turned on. This will assure ZVS turn on of the main MOSFETs. The time required for v_C to make this transition from 0 V to V_{in}, t_{ZVS}, can also be found out from (8) with the boundary condition of $v_C(t_{ZVS}) = V_{in}$. In order to clinch ZVS turn on of the main MOSFETs t_{ZVS} should be less than t_{db}. It should be noted that the node capacitance C_D is a voltage dependent nonlinear capacitor and hence to get accurate estimation, (5) and (6) have to be solved numerically, or C_D has to replaced by an equivalent linear capacitance $C_{D,eq}$, as presented in [17].

The rms and average current in the auxiliary MOSFETs and diodes and their reverse blocking voltage can be calculated by

$$I_{aux\_rms}=n_T I_{ZVS}\sqrt{\frac{2\varphi}{3\pi}}, \quad I_{aux\_avg}=n_T I_{ZVS}\frac{\varphi}{\pi}, \quad V_{aux}=\frac{V_{in}}{2n_T}. \quad (10)$$

Device ratings for auxiliary circuit can be decided from (10). The conduction losses in the auxiliary circuit of Fig. 3(a) is given by

$$P_{cond}=\frac{I_{ZVS}^2}{3}\frac{2\varphi}{\pi}(n_T^2R_{DS\_ON}+R_{ZVS})+I_{ZVS}\frac{\varphi}{\pi}n_TV_D, \quad (11)$$

where, R_{DS_ON} is the on state resistance of the auxiliary MOSFETs, V_D is the on state drop of the auxiliary diodes, R_{ZVS} is the effective series resistance of the ZVS assisting current carrying path which includes C_{ZVS} and the auxiliary transformer. The turn on loss of each of the auxiliary MOSFETs due to the energy stored in its output capacitance (C_{OSS}) can be given by

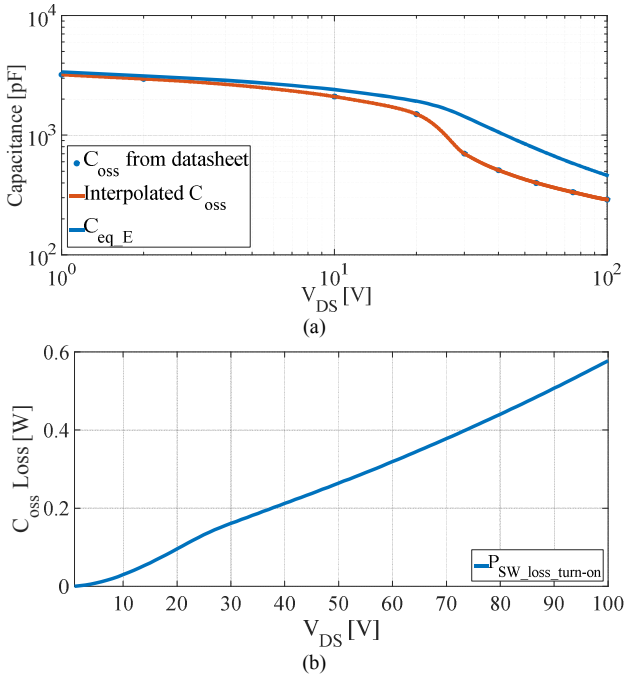

Fig. 5. (a) Output capacitance of the auxiliary MOSFET [orange] and its energy equivalent linear capacitor [blue] versus drain to source voltage (V_{DS}) of the MOSFET, (b) turn on energy lost from the stored energy in the output capacitor of the MOSFET versus V_{DS}.

$$P_{SW\_loss\_turn-on}=\frac{1}{2}C_{eq,E}\left(\frac{V_{in}}{2n_T}\right)^2 f_s, \quad (12)$$

where, $C_{eq,E}$ is the energy equivalent linear output capacitor [17] of the auxiliary MOSFET. Fig. 5(a) shows the C_{OSS} and $C_{eq,E}$ with respect to V_{DS} of the MOSFET (part number: FDB110N15A) and Fig. 5(b) shows the turn on loss in each of the auxiliary MOSFET for different V_{DS}.

IV. Experimental Results

A prototype of the SRC operating at 250 kHz has been developed with the parameters shown in Table I. The hardware setup of a SRC is shown in Fig. 6(a) whereas the ZVS assisting circuit is shown in Fig. 6(b). The auxiliary transformer used in the ZVS assisting circuit is a 5:1:1 transformer whose leakage inductance is used as L_{ZVS}.

Hardware test results at ~50% load and full load are shown in Fig. 7 where the SRC is operated from a 1 A DC current source and its output is regulated at 0.33 A with 1 kΩ and 2 kΩ load resistance, respectively. In Fig. 7, yellow trace (CH1) is the gate to source voltage for top MOSFET in leg A, light blue trace (CH2) is the primary side inverter voltage (v_{AB}), purple waveform (CH3) is the current in the resonant tank (i_{tank}) and the current in the ZVS assisting branch (i_{ZVS}) is shown by the green trace (CH4). From these results it can be

TABLE I
PARAMETERS OF THE CONVERTER

Parameter	Value
L_r (μH)	174.2
C_r (nF)	2.33
f_s (kHz)	250
n	2
I_g (A)	1
I_{out} (A)	0.33
P_{Load} (W)	0 – 250
n_T	5
L_{ZVS} (μH)	15
Q_{11}, Q_{12}	FDB110N15A
D_{11}, D_{12}	STB15200TR
Q_1, - Q_4	C2M1000170D

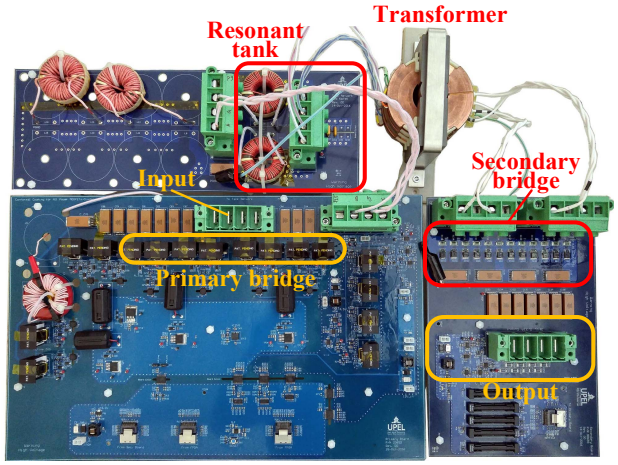

(a)

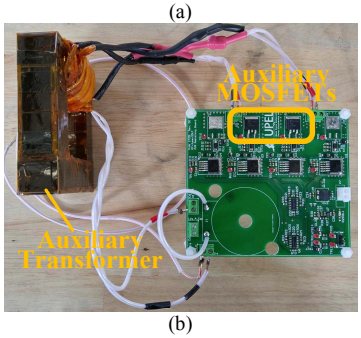

(b)

Fig. 6. (a) Photograph of the SRC hardware and (b) the ZVS assisting circuit.

seen that at the positive rising edge of v_{AB}, the voltage waveform reaches V_{in} before the gate of the top MOSFET in leg A is turned on confirming ZVS turn on. Figure 8 shows another set of waveforms of the converter operating at full load, where yellow trace (CH1) is the gate to source voltage of auxiliary MOSFET Q_{11}, the light blue trace (CH2) is the voltage across drain to source of Q_{11}, purple waveform (CH3) is the current in the resonant tank and green waveform (CH4) is the current in the ZVS assisting branch. It can be observed from Fig. 8, that the auxiliary switches turn on and off at zero current and the auxiliary MOSFET Q_{11} turns on with voltage across its drain to source of ~35 V while the V_{in} at this operating condition is ~250 V, which results in lower turn on voltage across the auxiliary MOSFETs and hence lower *dv/dt*.

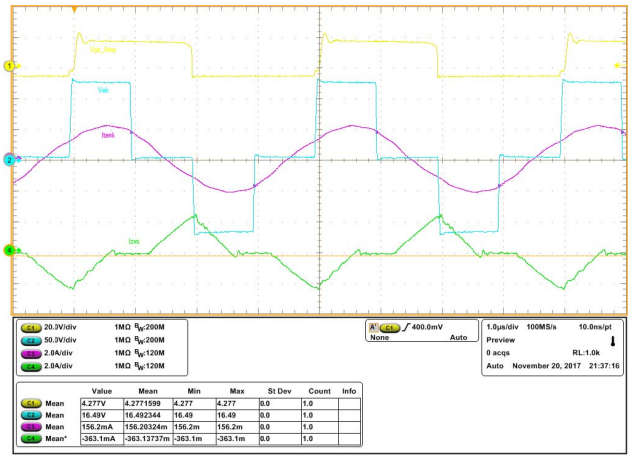

(a)

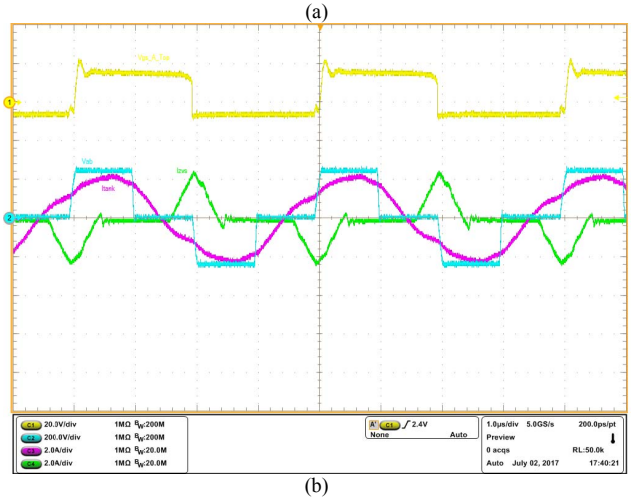

(b)

Fig. 7. Operating waveform of the SRC with the proposed ZVS assisting circuit at ~50% load.(a) and at full load (b). Yellow trace (CH1) is the gate to source voltage of top MOSFET in leg A, light blue (CH2) is the inverter output voltage v_{AB}, purple trace (CH3) is the tank current and green waveform (CH4) is the current in the assisting branch.

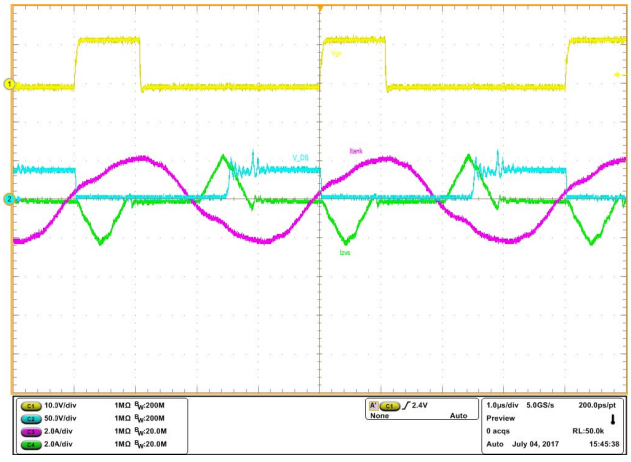

Fig. 8. Operating waveform of the SRC with the proposed ZVS assisting circuit at full load of 250 W, yellow waveform (CH1) is the gate-source voltage of auxiliary MOSFET Q_{11}, light blue (CH2) is the voltage across drain to source of Q_{11}, purple trace (CH3) is the tank current and green (CH4) is the current in the assisting branch.

V. CONCLUSION

For a constant current input DC-DC SRC, achieving ZVS for the full load range is challenging to realize using passive techniques. Conventional active ZVS techniques either increase the rms current in the main and auxiliary switches, leading to high conduction loss or have high voltage across the auxiliary switches at turn on which results in high *dv/dt* and EMI. In this paper, a multi-winding transformer based ZVS assisting circuit is proposed which has low rms current in the assisting branch as well as the main switching leg and at the same time lower voltage stress across the auxiliary switches. The leakage inductance of the auxiliary transformer is utilized as the ZVS assisting inductor so that no additional inductor is needed. Equivalent circuits of the ZVS assisting branch, during transition, is developed along with calculations showing the desired rating of the components required to realize the proposed circuit. Hardware prototype has been built to test the circuit operation at different loads. The waveforms obtained from hardware testing verifies the proposed circuit operation The proposed ZVS assisting circuit can be used in conjunction with any voltage fed half bridge switching leg to realize ZVS turn on of the switches.

REFERENCES

[1] H. Wang, T. Saha, R. Zane, "Design Considerations for Series Resonant Converters with Constant Current Input," *2016 IEEE Energy Conversion Congress and Exposition (ECCE)*, Milwaukee, WI, 2016, pp. 1-8.

[2] H. Wang, T. Saha and R. Zane, "Analysis and design of a series resonant converter with constant current input and regulated output current," *2017 IEEE Applied Power Electronics Conference and Exposition (APEC)*, Tampa, FL, 2017, pp. 1741-1747.

[3] N. Hasan, H. Wang, T. Saha and Z. Pantic, "A novel position sensorless power transfer control of lumped coil-based in-motion wireless power transfer systems," *Energy Conversion Congress and Exposition (ECCE)*, pp. 586-593, Sept. 2015.

[4] Y. Shang, N. Cui, Q. Zhang and C. Zhang, "A battery equalizer with zero-current switching and zero-voltage gap among cells based on three-resonant-state LC converters," *2017 IEEE Applied Power Electronics Conference and Exposition (APEC)*, Tampa, FL, 2017, pp. 1647-1651.

[5] I. Zeltser, O. Kirshenboim, N. Dahan and M. M. Peretz, "ZCS resonant converter based parallel balancing of serially connected batteries string," 2016 IEEE Applied Power Electronics Conference and Exposition (APEC), Long Beach, CA, 2016, pp. 802-809.

[6] H. Chen and D. Divan, "High speed switching issues of high power rated silicon-carbide devices and the mitigation methods," 2015 IEEE Energy Conversion Congress and Exposition (ECCE), Montreal, QC, 2015, pp. 2254-2260.

[7] A. Safaee, P. Jain and A. Bakhshai, "A ZVS Pulsewidth Modulation Full-Bridge Converter With a Low-RMS-Current Resonant Auxiliary Circuit," in *IEEE Transactions on Power Electronics*, vol. 31, no. 6, pp. 4031-4047, June 2016.

[8] A. Safaee, M. Karimi-Ghartemani, P. K. Jain and A. Bakhshai, "Time-Domain Analysis of a Phase-Shift-Modulated Series Resonant Converter with an Adaptive Passive Auxiliary Circuit," in *IEEE Transactions on Power Electronics*, vol. 31, no. 11, pp. 7714-7734, Nov. 2016.

[9] T. Saha, H. Wang, B. Riar and R. Zane, "Analysis of zero voltage switching requirements and passive auxiliary circuit design for DC-DC series resonant converters with constant input current," *2016 IEEE 2nd Annual Southern Power Electronics Conference (SPEC)*, Auckland, 2016, pp. 1-6.

[10] R. W. De Doncker and J. P. Lyons, "The auxiliary resonant commutated pole converter," *Industry Applications Society Annual Meeting, 1990., Conference Record of the 1990 IEEE*, Seattle, WA, USA, 1990, pp. 1228-1235 vol.2.

[11] J. G. Cho, J. A. Sabate and F. C. Lee, "Novel full bridge zero-voltage-transition PWM DC/DC converter for high power applications," *Applied Power Electronics Conference and Exposition, 1994. APEC '94. Conference Proceedings 1994., Ninth Annual*, Orlando, FL, 1994, pp. 143-149 vol.1.

[12] M. Yaqoob, K. H. Loo and Y. M. Lai, "A switched-inductor-augmented resonant DAB converter for achieving wide-range zero voltage switching," *2016 IEEE 7th International Symposium on Power Electronics for Distributed Generation Systems (PEDG)*, Vancouver, BC, 2016, pp. 1-7.

[13] L. Corradini, D. Seltzer, D. Bloomquist, R. Zane, D. Maksimović and B. Jacobson, "Zero Voltage Switching Technique for Bidirectional DC/DC Converters," in *IEEE Transactions on Power Electronics*, vol. 29, no. 4, pp. 1585-1594, April 2014.

[14] T. Saha, H. Wang and R. Zane, "Zero voltage switching assistance design for DC-DC series resonant converter with constant input current for wide load range," *2017 IEEE 18th Workshop on Control and Modeling for Power Electronics (COMPEL)*, Stanford, CA, 2017, pp. 1-5.

[15] W. Han and L. Corradini, "Accurate ZVS boundary analysis for bidirectional dual-bridge series resonant dc-dc converters," *2017 IEEE 18th Workshop on Control and Modeling for Power Electronics (COMPEL)*, Stanford, CA, 2017, pp. 1-8.

[16] U. Kundu, K. Yenduri and P. Sensarma, "Accurate ZVS Analysis for Magnetic Design and Efficiency Improvement of Full-Bridge LLC Resonant Converter," *in IEEE Transactions on Power Electronics*, vol. 32, no. 3, pp. 1703-1706, March 2017.

[17] D. Costinett, D. Maksimović and R. Zane, "Circuit-Oriented Treatment of Nonlinear Capacitances in Switched-Mode Power Supplies," in *IEEE Transactions on Power Electronics*, vol. 30, no. 2, pp. 985-995, Feb. 2015.